New Physics: Sae Mulli,
Vol. 70, No. 12, December 2020, pp. 1085∼1091
http://dx.doi.org/10.3938/NPSM.70.1085

α + ^{116}Sn and ^{6}Li + ^{116}Sn Elastic Scatterings at E_{lab} = 240 MeV : Coulomb-modified Glauber Model Approach

Yong Joo KIM*
Department of Physics, Jeju National University, Jeju 63243, Korea

(Received 22 September 2020 : accepted 10 November 2020)

We analyzed experimental data on elastic α + ^{116}Sn and ^{6}Li + ^{116}Sn scatterings at E_{lab} = 240 MeV within the framework of the Coulomb-modified Glauber model. The ingredients of the model used in this work were the nucleon-nucleon (NN) amplitude and the densities of the colliding nuclei. The calculations included the effective NN amplitude considering a q^4 component and the surface-matched Gaussian density of the target nucleus. The calculated results reproduced satisfactorily the structures of differential cross sections and agreed well with the experimental data. The oscillatory structures observed in the angular distributions were explained using the strong interference between the near-side and the far-side scattering amplitudes. We found that the introduction of both an effective NN amplitude and a surface-matched Gaussian density plays an important role in providing a better description of the elastic data.

Keywords: Coulomb-modified Glauber model, Effective NN amplitude, Surface-matched Gaussian density, Elastic scattering, α + ^{116}Sn, ^{6}Li + ^{116}Sn

I. Introduction

Over the years, a number of efforts [1–7] have been made to describe the scattering processes between heavy-ions in terms of the optical limit approximation (OLA) to the Glauber model. Although the OLA takes a first (leading) term in the expansion of the phase shift function, it gives a reasonable account of the elastic scattering data at high energies. The basic point of the OLA is that the projectile follows a straight line trajectory characterized by the impact parameter b during the collision with the target nucleus. At relatively low and intermediate energies, this trajectory is modified [2] to account for the deviation in the straight line trajectory of the Glauber model because of the Coulomb field. This type of OLA to the Glauber model is usually called as "Coulomb-modified Glauber model(CMGM)".

In determining the nuclear phase shift in CMGM, the nuclear density and nucleon-nucleon (NN) amplitude are the basic inputs. It is well known that analytic phase shift form [1, 2] can be obtained by assuming the nuclear density distribution to be Gaussian form. Most of the work reported has been done using Gaussian density. This assumption is suitable for the light nucleus ($A < 40$). For the heavy nucleus ($A \geqq 40$), the realistic density form such as Fermi shape, which allows for a tapered density distribution at the nuclear surface, is required.

To use the analytic OLA phase shift for the analysis of elastic cross section, it is necessary to extract the Gaussian density parameters from the matching between the Gaussian and realistic density distributions in the nuclear surface. Karol [8] reported the Gaussian density parameters by matching procedure. Meanwhile, the CMGM using effective NN amplitude (ENNA) taking account of the higher q (q is the momentum transfer) has been used to get a better description of the experimental data having wide range of scattering angle. The ENNA has been applied [9] successfully to the α+ nucleus elastic scattering in the energy range 25 – 70 MeV/nucleon.

*E-mail: yjkim@jejunu.ac.kr

An analysis of the 240 MeV alpha particle elastic scatterings on ^{58}Ni, ^{116}Sn and ^{197}Au targets has been made [10] within the framework of CMGM using an effective $N-\alpha$ amplitude. In our previous papers [11,12], we presented a CMGM using an effective NN amplitude taking account of a q^4 component and it has been satisfactorily applied to $\alpha+$ ^{16}O elastic scatterings at $E_{lab}=$ 240 and 400 MeV. The CMGM with surface-matched Gaussian density (SMGD) was employed to analyze the 240 MeV alpha particle elastic scatterings on ^{40}Ca and ^{58}Ni targets.

The experimental data for the elastic scatterings of 240 MeV alpha particle and ^{6}Li beam on ^{116}Sn target have been reported [13,14]. The data were compared with a calculation using optical and folding models. In this paper, we attempt a CMGM calculation for the differential cross sections of the $\alpha+$ ^{116}Sn and ^{6}Li + ^{116}Sn elastic scatterings at $E_{lab}=$ 240 MeV using both the ENNA taking account a q^4 and SMGD for the target nucleus ^{116}Sn. The calculations will be compared to the ones without SMGD. Comparisons of the results obtained from conventional and effective NN amplitudes will also be made. Further, the near-side and far-side decompositions following the Fuller formalism [15] will be performed to understand the structure of differential cross section. In the following section, we describe a CMGM theory related with the ENNA and surface-matched Gaussian density. In Sec. III, the results and discussion of $\alpha+$ ^{116}Sn and ^{6}Li + ^{116}Sn are presented. The concluding remarks are given in Sec. IV.

II. Theoretical Framework

1. Coulomb-modified Glauber model

In the case of nucleus-nucleus elastic scattering, the nuclear phase shift $\delta(b)$ of OLA may be expressed as [16, 17]

$$\delta(b)=\frac{A_PA_T}{2k_{NN}}\int_0^\infty dqqJ_0(qb)f_{NN}(q)F_P(q)F_T(q), \quad (1)$$

where q and k_{NN} denote the momentum transfer and the incident momentum of nucleon in the center of mass system, $f_{NN}(q)$ is NN scattering amplitude. And $F_{P/T}(q)$ are the form factors related with the projectile (P) and target (T) densities. By assuming a Gaussian density of the form

$$\rho_i(r)=\rho_i(0)\exp(-\frac{r^2}{a_i^2}),\ i=P,T \quad (2)$$

the nuclear form factor $F_i(q)$ can be calculated from the Fourier transforms of the $\rho_i(r)$ as following :

$$F_i(q)=(\sqrt{\pi}a_i)^3\rho_i(0)\exp(-q^2a_i^2/4). \qquad i=P,T \quad (3)$$

In order to account for elastic data covering large scattering angles, we take a parametrized form of $f_{NN}(q)$ that used in [9,10]

$$f_{NN}(q)=\frac{k_{NN}}{4\pi}\sigma_{NN}(\varepsilon_{NN}+i)\exp(-\beta_{NN}q^2/2)[1+\lambda q^4], \quad (4)$$

where σ_{NN}, ε_{NN} and β_{NN} are the values of NN total cross section, the ratio of real to imaginary parts of the forward NN scattering amplitude and the slope parameter, respectively. And λ is the free fitting parameter. This form of $f_{NN}(q)$ is the effective NN amplitude (ENNA), while the conventional NN amplitude (CNNA) has the form with $\lambda=0$ in Eq. (4). Inserting Eqs. (3)-(4) into Eq. (1), the nuclear phase shift $\delta(b)$ can be written as a form

$$\begin{aligned}\delta(b)=&\frac{A_PA_T}{4R^2}\pi^2a_P^3a_T^3\rho_P(0)\rho_T(0)\sigma_{NN}(\varepsilon_{NN}+i)\\&\times[1+\lambda\frac{16}{R^4}(2-\frac{4b^2}{R^2}+\frac{b^4}{R^4})]\exp[-\frac{b^2}{R^2}]\end{aligned} \quad (5)$$

with

$$R^2=a_P^2+a_T^2+2\beta_{NN}. \quad (6)$$

The CMGM usually adopted the distance of closest approach r_c instead of impact parameter $b=\sqrt{L(L+1)}/k$ in Eq. (5) because of the Coulomb field, as suggested in Ref. [2]. The quantity r_c is given as

$$r_c=\frac{1}{k}(\eta+\sqrt{\eta^2+L(L+1)}) \quad (7)$$

where k is the momentum of nucleus-nucleus system and η the Sommerfeld parameter. By replacing b in $\delta(b)$ by r_c, the nuclear phase shift can be evaluated in terms of r_c.

The elastic differential scattering cross section $d\sigma/d\Omega$ is given by

$$\frac{d\sigma}{d\Omega}=|f(\theta)|^2, \quad (8)$$

where the scattering amplitude $f(\theta)$ for nonidentical spinless nuclei is taken as the form

$$f(\theta) = f_R(\theta) + \frac{1}{ik}\sum_{L=0}^{\infty}(L+\frac{1}{2})\exp(2i\sigma_L)(S_L-1)P_L(\cos\theta). \quad (9)$$

Here $f_R(\theta)$, σ_L and $P_L(\cos\theta)$ are, respectively, the Rutherford scattering amplitude, the Coulomb phase shift and the Legendre polynomial. The nuclear $S-$matrix elements S_L in this equation can be expressed by using the nuclear phase shift $\delta(r_c)$ so that :

$$S_L = \exp(2i\delta(r_c)). \quad (10)$$

2. Calculations of Gaussian density parameters

We have assumed that the nuclear density for the light nuclei ($A < 40$) has the Gaussian form of Eq. (2). The two parameters a_i and $\rho_i(0)$ in Eq. (2) are related to the root-mean-square (RMS) radius $< r_i^2 >^{1/2}$ of the nucleus by the relation [1]

$$a_i = \frac{< r_i^2 >^{1/2}}{\sqrt{1.5}}, \quad \rho_i(0) = \frac{1}{(a_i\sqrt{\pi})^3}, \quad i = P, T \quad (11)$$

where the density is assumed to be normalized to unity. In the case of heavy nuclei having mass numbers larger than 40, realistic nuclear density is required to reproduce surface which sensitive to the elastic scattering. As mentioned in previous subsection, the phase shift Eq. (5) is derived by assuming both the projectile and target densities as Gaussian form. To use the analytic expression of phase shift Eq. (5), the Gaussian density parameters a_T and $\rho_T(0)$ for target nucleus are adjusted by matching the Gaussian density distribution to the realistic density one in nuclear surface.

The realistic two-parameter Fermi (2pF) density for target nucleus can be written as

$$\rho_T^{2pF}(r) = \frac{\rho_T^{2pF}(0)}{1+\exp[(r-c_T)/d_T]}, \quad (12)$$

where

$$\rho_T^{2pF}(0) = \left[4\pi\int_0^{\infty}\frac{1}{1+\exp[(r-c_T)/d_T]}\right]^{-1}. \quad (13)$$

Table 1. Values of parameters entering in Eq. (5), χ^2/N and reaction cross section σ_R values in the Coulomb-modified Glauber model using the effective NN amplitude for the elastic scattering of 240 MeV α and ^{6}Li on ^{116}Sn. Cal. 1 and Cal. 2 are the values obtained by using the non-SMGD and SMGD, respectively. The χ^2/N and σ_R values denote the results using the effective (conventional) NN amplitude. 10% error bars are adopted to obtain χ^2/N values.

System	α + ^{116}Sn		^{6}Li + ^{116}Sn	
	Cal. 1	Cal. 2	Cal. 1	Cal. 2
$\rho_P(0)(fm^{-3})$	0.0659817	0.0659817	0.0209889	0.0209889
$a_P(fm)$	1.39621	1.39621	2.04532	2.04532
$\rho_T(0)(fm^{-3})$	0.00333847	0.0225154	0.00333847	0.0225154
$a_T(fm)$	3.77493	2.90637	3.77493	2.90637
$\sigma_{NN}(mb)$	62.33	62.33	98.52	98.52
$\beta_{NN}(fm^2)$	0.91495	0.91495	0.7725	0.7725
ε_{NN}	1.572	1.108	0.340	0.553
$\lambda(fm^4)$	0.475+0.550i	0.218-0.201i	1.299-2.093i	0.318-0.559i
χ^2/N	20.06 (22.80)	4.98 (10.87)	33.21 (42.13)	12.85 (98.29)
$\sigma_R(mb)$	2584 (2381)	2144 (2147)	3146 (3005)	2718 (2712)

Karol [8] calculated the Gaussian density parameters $\rho_T(0)$ and a_T by matching the 2pF density in the surface, and these parameters are given as

$$\rho_T(0) = \frac{1}{2}\rho_T^{2pF}(0)\exp(\frac{c_T^2}{a_T^2}) \quad (14)$$

and

$$a_T = \left[\frac{4c_T t + t^2}{4(\ln 5)}\right]^{1/2}, \quad (15)$$

where $t = 4.4d_T$ is the 90% - 10% surface skin thickness parameter.

To get the SMGD parameters for ^{116}Sn nucleus, we used $c_T = 5.433\ fm$ and $d_T = 0.515\ fm$ as the 2pF density parameters taken from Ref. [13]. Table 1 lists the values of the Gaussian density parameters a_T and $\rho_T(0)$ for ^{116}Sn nucleus, along with the ones determined by RMS radii. Density distributions for ^{116}Sn nucleus are illustrated in Fig. 1. The solid curve corresponds to the 2pF density distribution and the dotted curve the surface-matched Gaussian density one. As this figure shows, the agreement between two curves is good in surface region. Since the surface regions of colliding nuclei play a key role in determining the elastic scattering cross section, the discrepancies between the realistic 2pF density and the surface-matched Gaussian one at the central regions are not important.

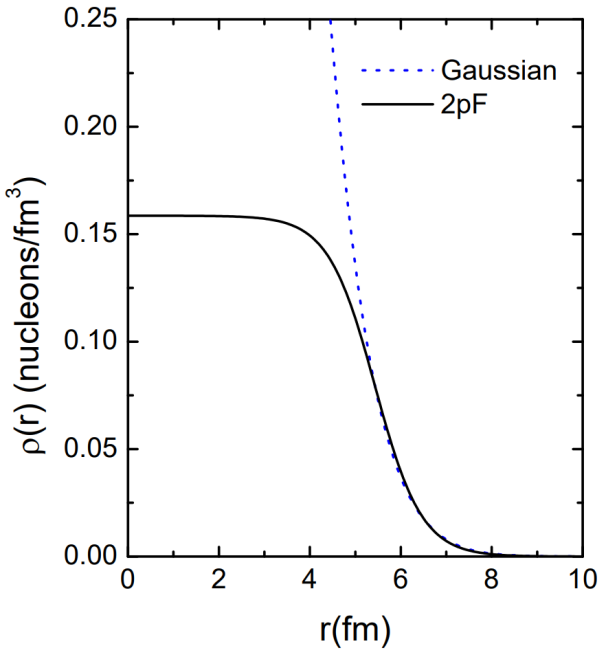

Fig. 1. (Color online) Two-parameter Fermi (solid curve) and Gaussian (dotted curve) density distributions for ^{116}Sn nucleus. The density distribution is normalized to the mass number of the nucleus.

3. Determination of input parameters

To analyze the elastic data for α + ^{116}Sn and ^{6}Li + ^{116}Sn systems at E_{lab} = 240 MeV, we used the CMGM using the ENNA and surface-matched Gaussian density of target nuclei. The inputs needed to calculate the elastic cross sections are the parameters included in the Gaussian density ($\rho_P(0)$, $\rho_T(0)$, a_P and a_T) and NN scattering amplitude (σ_{NN}, ε_{NN}, λ and β_{NN}). The input parameters are determined as follows :

(1) The Gaussian density parameters $\rho_P(0)$ and a_P for projectiles (α and ^{6}Li) were obtained from Eq. (11) with RMS radius [3,18].

(2) For the target nucleus (^{116}Sn), two different Gaussian density parameters are considered. The first type is calculated from RMS radius $< r_T^2 >^{1/2}$ defined as

$$< r_T^2 >^{1/2} = \left(\frac{4\pi \int_0^\infty \rho_T^{2pF}(r) r^4 dr}{4\pi \int_0^\infty \rho_T^{2pF}(r) r^2 dr} \right)^{1/2} . \qquad (16)$$

The second type is from surface-matched method given by Eqs. (14) and (15).

(3) The NN total cross sections σ_{NN} were calculated from Eqs. (22) – (23) and (25) of Ref. [3] and Eq. (2) of Ref. [19] with $\rho = 0.23\ fm^{-3}$ [9].

(4) The values of slope parameter β_{NN} were taken as an average of $\beta_{pp(nn)}$ and $\beta_{np(pn)}$ given in Tables 2 and 5 of Ref. [9].

(5) The ε_{NN} and λ were considered as adjustable parameters determined from minimizing the $\chi^2/N-$value (N is the numbers of experimental points).

III. Results and Discussion

1. Elastic cross sections using conventional NN amplitude

First, the Coulomb-modified Glauber model using CNNA ($\lambda = 0$ in Eq. (4)) is used to carry out searching the parameter ε_{NN} whose value yields the minimized $\chi^2/N-$value for elastic scattering data. The determined ε_{NN} values are given in Table 1. Based on the CMGM with CNNA, calculations have been made with two types of Gaussian density parameters for the ^{116}Sn nucleus. The results of calculations for α + ^{116}Sn and ^{6}Li + ^{116}Sn differential cross section at 240 MeV are displayed in Fig. 2. The solid curves denote the calculated results obtained with the SMGD parameters Eqs. (14) and (15), while the dotted curves are the ones obtained by using the Gaussian densities Eq. (11) with $< r_T^2 >^{1/2}$= 4.62333 fm for the ^{116}Sn nucleus. Here the RMS radius $< r_T^2 >^{1/2}$ of ^{116}Sn was determined from Eq. (16) with 2pF density distribution given in Eq. (12) having $c_T = 5.433 fm$ and $d_T = 0.515 fm$ [13]. The solid circles show the experimental data taken from the works of Clark *et al.* [13] (for α + ^{116}Sn) and Chen *et al.* [14] (for ^{6}Li + ^{116}Sn). For α + ^{116}Sn system, the solid curve yielded reasonable descriptions of the elastic scattering data, while dotted curve differed greatly from the observed data especially at large angle regions. In the case of ^{6}Li + ^{116}Sn system, dotted curve generated the structureless decreasing pattern and did not reproduced the observed data. On the contrary, the solid curve of Fig. 2(b) reproduced qualitative trend (refractive oscillations) of experimental angular distributions in spite of large χ^2/N value. It can be said that the adoption of SMGD is important in providing a better description of elastic data involved the heavier nucleus.

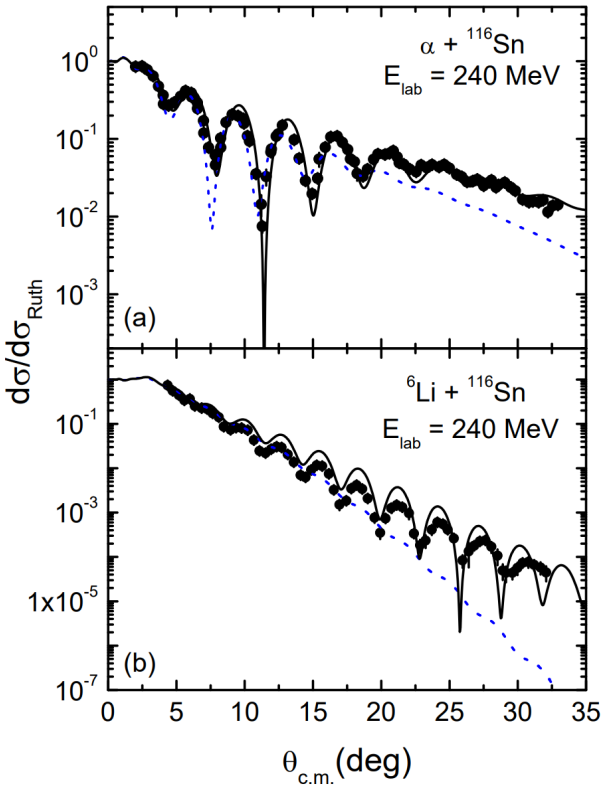

Fig. 2. (Color online) Measured data (solid circles) [13, 14] for α + ^{116}Sn and ^{6}Li + ^{116}Sn elastic scatterings at E_{lab} = 240 MeV, and Coulomb-modified Glauber model fits to them. The solid and dotted curves are the calculations obtained by using the conventional NN amplitude with SMGD and non-SMGD, respectively.

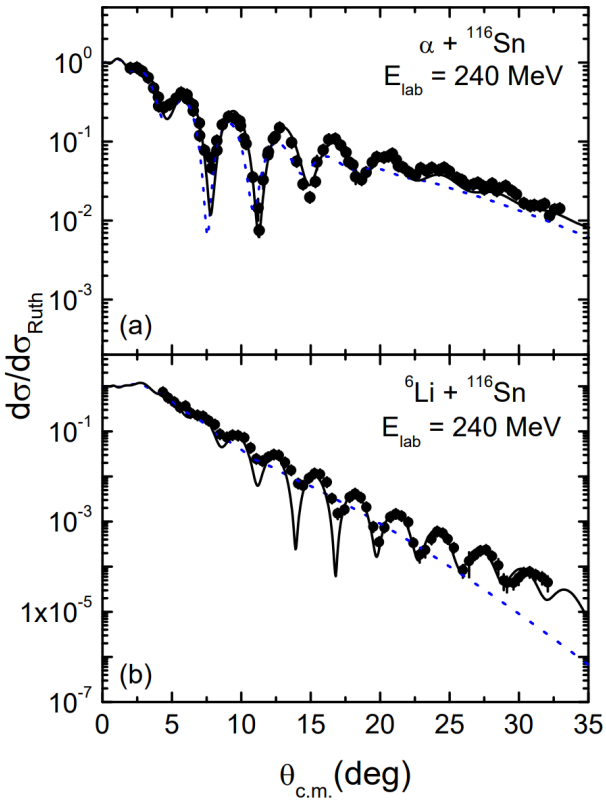

Fig. 3. (Color online) Measured data (solid circles) [13, 14] for α + ^{116}Sn and ^{6}Li + ^{116}Sn elastic scatterings at E_{lab} = 240 MeV, and Coulomb-modified Glauber model fits to them. The solid and dotted curves are the calculations obtained by using the effective NN amplitude with SMGD and non-SMGD, respectively.

2. Elastic cross sections using effective NN amplitude

Apparently the calculations using CNNA do not provide a satisfactory description of the experimental data of two system. Thus, we have performed CMGM calculations using ENNA to get better agreements with the experimental data. After fixing the parameter ε_{NN} value determined from CNNA, we searched the parameter λ included in ENNA that provides lowest $\chi^2/N-$values for elastic data. The determined λ values are also listed in Table 1. The calculations using the effective NN amplitude are shown in Fig. 3(a) (for α + ^{116}Sn) and 3(b) (for ^{6}Li + ^{116}Sn), together with the experimental data. The solid and dotted curves correspond to the results obtained with and without SMGD, respectively. The solid curves of Fig. 3(a) and (b) agree fairly well with the experimental data. This is also evident from small $\chi^2/N-$values. On the other hand, the dotted curve of Fig. 3(a) provided poor fits to the large angle cross sections of α + ^{116}Sn system, although it has reasonable success with the elastic data only up to about $\theta_{c.m.} < 12$. For ^{6}Li + ^{116}Sn scattering, dotted curve generated smooth exponential falloff pattern as shown in Fig. 3(b), consequently did not provided the refractive oscillatory structures observed in this system. This poor fit is also reflected by the large χ^2/N values. As a matter of fact, the CMGM calculations (solid curves in Fig. 3) using both the ENNA and SMGD greatly enhanced the agreements with the experimental data.

3. Near-far decomposition

The structure of angular distribution can be understood by the decomposition of the elastic scattering amplitude into the far-side and the near-side components

within the approach of Fuller [15] The effective NN amplitude and SMGD were used in the CMGM calculation for differential, far-side and near-side elastic cross sections. Fig. 4 shows the differential cross sections (solid curves), their far-side (dashed curves) and near-side (dotted curves) components for α + ^{116}Sn and ^{6}Li + ^{116}Sn systems at E_{lab} = 240 MeV. We note that the near-side component contributes dominantly to the forward-angle cross section, where the far-side contributions are negligible. But the far-side amplitude arising from nuclear attraction becomes important with increasing the scattering angle. The enhanced far-side amplitude strongly interferes with the near-side one, consequently leading to oscillatory structure in the elastic differential cross section. The elastic angular distributions due to the near/far-side amplitudes are found to be nearly same magnitude at the crossing angles $\theta_{cross} = 9.5^{o}$ for α + ^{116}Sn and $\theta_{cross} = 15.4^{o}$ for ^{6}Li + ^{116}Sn systems, respectively. The maximum amplitude of interference oscillations are observed around θ_{cross}. The structureless smooth pattern of large angle cross section in the α + ^{116}Sn system can be interpreted as scattering from the dominance of far-side component. However, in the case of ^{6}Li + ^{116}Sn system, the near-side component has considerable (non-negligible) magnitude at large angle regions. The small oscillatory behavior of large angle cross section can be explained as being arose from the weak interference between near-side and far-side amplitudes.

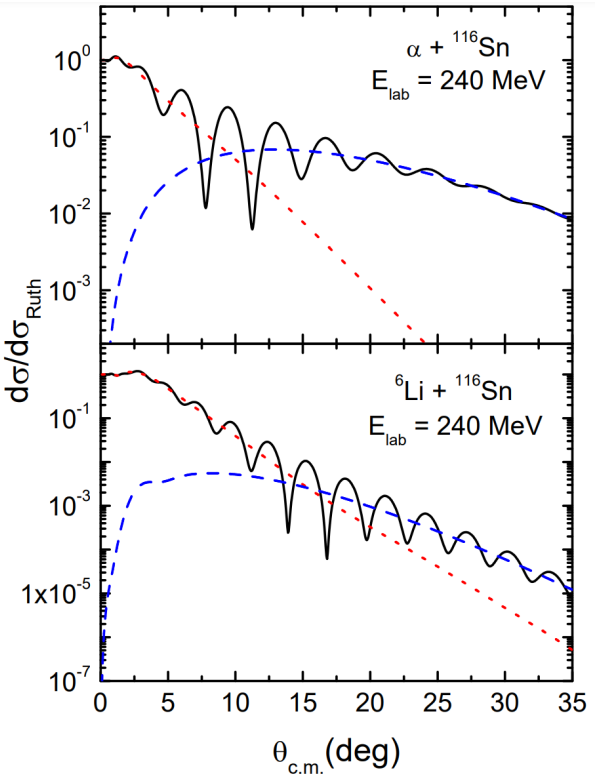

Fig. 4. (Color online) Differential cross sections (solid curves) for α + ^{116}Sn and ^{6}Li + ^{116}Sn elastic scatterings at E_{lab} = 240 MeV, their far-side (dashed curves) and near-side (dotted curves) components following the decomposition procedure of Fuller [15]. All calculations are obtained by using the Coulomb-modified Glauber model with both the ENNA and SMGD.

IV. Concluding Remarks

In this paper, we have analyzed the α + ^{116}Sn and ^{6}Li + ^{116}Sn elastic scatterings at E_{lab} = 240 MeV using the Coulomb-modified Glauber model. The main feature of the present study is the use of the ENNA and surface-matched Gaussian density of target. The CNNA was first employed to determine the parameter ε_{NN} from fitting the elastic data. From the calculated results using CNNA, we can see the followings : (1) The results calculated from non-surface-matched Gaussian density reproduce the experimental data only up to about $\theta_{c.m.} < 12^{o}$ and yield poor fits to the large angle cross section data of α + ^{116}Sn system. Further, the calculation for ^{6}Li + ^{116}Sn system generates a simple decreasing shape, and does not reproduce the refractive oscillatory structures appearing in elastic angular distributions. (2) The calculated results for the α + ^{116}Sn system using the surface-matched Gaussian density give somewhat a reasonable fit to the elastic data. And for ^{6}Li + ^{116}Sn system, this calculation provides a qualitative trend (refractive oscillations) of experimental angular distributions in spite of large χ^2/N value. Consequently, it can be said that the adoption of SMGD plays a role in providing a better description of the experimental elastic data involving heavy nucleus.

In order to get better agreements with the experimental data, the calculations have been made with the effective NN amplitude. After fixing the parameter ε_{NN} value determined from CNNA, we searched the parameter λ involved in effective NN amplitude by using the least-square method. From a ENNA perspective, we can find the followings : (1) For α + ^{116}Sn, the calculation with non-surface-matched Gaussian density gives

the poor quality fit to the data especially at large angles, though it provide a acceptable fit to elastic data only up to about $\theta_{c.m.} < 12^{o}$ like as the results from CNNA. In the case of ^{6}Li + ^{116}Sn system, this calculation generates smooth exponential falloff pattern, which greatly differs from the experimental angular distribution. (2) When the SMGD is used, the result for α + ^{116}Sn provides more satisfactory fits to the elastic data (lower $\chi^2/N-$value), in comparison with the results using non-SMGD. Also, the calculation for ^{6}Li + ^{116}Sn system reproduces well the characteristic refractive oscillation pattern observed and gives reasonable fit to the experimental data. Finally, under the consideration of both the ENNA and the surface-matched Gaussian density, Coulomb-modified Glauber model calculations reproduced fairly well the elastic data for α + ^{116}Sn and ^{6}Li + ^{116}Sn systems at E_{lab} = 240 MeV.

Through a decomposition of elastic scattering amplitude in terms of the near-side and the far-side component, we can see that the oscillatory patterns observed on the elastic angular distributions of α + ^{116}Sn and ^{6}Li + ^{116}Sn systems were arose from interference between the two scattering amplitudes. The maximum amplitudes of interference oscillations are occurred around the crossing angles. The behaviors of large-angle cross section of α + ^{116}Sn system were almost completely reproduced by the far-side scattering. But weak oscillatory behaviors observed at large angles of ^{6}Li + ^{116}Sn system can be understood in terms of interference between the far-side and the considerable (non-negligible) near-side contributions to the elastic cross sections.

ACKNOWLEDGEMENTS

This research was supported by the 2020 scientific promotion program funded by Jeju National University.

REFERENCES

[1] J. Chauvin, D. Lebrun, A. Lounis and M. Buenerd, Phys. Rev. C **28**, 1970 (1983).
[2] A. Vitturi and F. Zardi, Phys. Rev. C **36**, 1404 (1987).
[3] S. K. Charagi and S. K. Gupta, Phys. Rev. C **41**, 1610 (1990).
[4] S. K. Gupta and P. Shukla, Phys. Rev. C **52**, 3212 (1995).
[5] P. Shukla, Phys. Rev. C **67**, 054607 (2003).
[6] M. Rashdan, Int. J. Mod. Phys. E **21**, 1250083 (2012).
[7] M. A. M. Hassan *et al.*, Int. J. Mod. Phys. E **24**, 1550062 (2015).
[8] P. J. Karol, Phys. Rev. C **11**, 1203 (1975).
[9] D. Chauhan and Z. A. Khan, Eur. Phys. J. A **41**, 179 (2009).
[10] M. A. Alvi, J. H. Madani and A. M. Hakmi, Phys. Rev. C **75**, 064609 (2007).
[11] Y. J. Kim, New Phys.:Sae Mulli **67**, 1312 (2017).
[12] Y. J. Kim, New Phys.:Sae Mulli **68**, 1324 (2018).
[13] H. L. Clark, Y. W. Lui and D. H. Youngblood, Phys. Rev. C **57**, 2887 (1998).
[14] X. Chen *et al.*, Phys. Rev. C **76**, 054606 (2007).
[15] R. C. Fuller, Phys. Rev. C **12**, 1561 (1975).
[16] I. Ahmad, M. A. Abdulmomen and M. A. Alvi, Int. J. Mod. Phys. E **11**, 519 (2002).
[17] I. Ahmad and M. A. Alvi, Int. J. Mod. Phys. E **13**, 1225 (2004).
[18] M. M. H. El-Gogary, A. S. Shalaby, M. Y. Hassan and A. M. Hegazy, Phys. Rev. C **61**, 044604 (2000).
[19] C. Xiangzhou *et al.*, Phys. Rev. C **58**, 572 (1998).